Temperature dependence of band gaps in Si and Ge

P. Lautenschlager, P. B. Allen,* and M. Cardona
Max-Planck-Institut für Festkörperforschung, Heisenbergstrasse 1, D-7000 Stuttgart 80, Federal Republic of Germany
(Received 17 September 1984)

We extend earlier calculations of the temperature dependence of the electronic states at the Γ point of Si and Ge to other points of the Brillouin zone. Thus we are able to calculate the temperature dependence of gaps and critical-point energies: the indirect gap and the E_1 and E_2 critical points, as well as the E_0 gap of Si and the E_0' gap of Ge. Both the Fan self-energy and the Debye-Waller terms of the electron-phonon interaction are included. The theoretical results, corrected for the contribution of thermal expansion to the temperature shifts, show satisfactory agreement with experimental data.

I. INTRODUCTION

The energy bands of semiconductors, and therefore the various absorption edges and interband critical points, exhibit large shifts with temperature at constant pressure. Two effects contribute to these shifts. The first is due to the thermal expansion of the lattice coupled with the change of the electron energies with volume. The second contribution is the direct renormalization of band energies by electron-phonon interactions.[1] The total shift can be expressed by the derivatives

$$\left[\frac{\partial E_g}{\partial T}\right]_p = \left[\frac{\partial E_g}{\partial T}\right]_V + \left[\frac{\partial E_g}{\partial T}\right]_{\text{therm exp}}, \tag{1}$$

with

$$\left[\frac{\partial E_g}{\partial T}\right]_{\text{therm exp}} = \left[\frac{\partial \ln V}{\partial T}\right]_p \left[\frac{\partial p}{\partial \ln V}\right]_T \left[\frac{\partial E_g}{\partial p}\right]_T$$

$$= -3\alpha B \left[\frac{\partial E_g}{\partial p}\right]_T, \tag{2}$$

where $\alpha = L^{-1}(\partial L/\partial T)_p$ is the thermal-expansion coefficient and $B = -V(\partial p/\partial V)_T$ is the bulk modulus. Hence the magnitude of the differential thermal-expansion shift can be calculated by means of experimental values for α, B, and $(\partial E_g/\partial p)_T$, where care of the fact that α is strongly dependent on T, and even reverses sign at low T, must be taken.

This paper presents theoretical calculations of the effect of the electron-phonon interaction on the temperature dependence of the bands for several absorption edges. Two types of electron-phonon interactions must be distinguished, the Debye-Waller terms[2] and the "self-energy" terms.[3] Both terms arise from a perturbative calculation[4] of the electron self-energy to second order in atomic displacement **u**. The Debye-Waller terms are obtained from the electron-phonon Hamiltonian of second order in **u**. The self-energy terms correspond to the first-order electron-phonon Hamiltonian taken in second-order perturbation theory. The coupling constants for the Debye-Waller terms depend only on the electronic state and not on the phonon under consideration. They are relatively easy to evaluate. The self-energy terms are different for each electronic state and phonon involved. Their evaluation requires tedious numerical integration for all phonons and all possible electronic intermediate states. This is the reason why the self-energy terms, proposed earlier by Fan,[3] have been ignored in most of the existing calculations of the temperature dependence of the band structure.

In a previous paper,[5] hereafter denoted II, calculations were performed for the temperature dependence of the lowest direct gaps of germanium (E_0 gap) and silicon (E_0' gap). In the present work we extend these calculations to transitions along the ⟨111⟩ directions (the E_1 critical points), and the E_2 critical points which contain most of the oscillator strength for interband transitions, as well as to the indirect gap, the E_0 gap of Si, and the E_0' gap of Ge. The results are compared with experimental values. For all investigated transitions, with the possible exception of the E_2 gap, which is not well localized in **k** space, we find a satisfactory agreement between theory and experiment.

II. THE MODEL

The same method is used as in II. Only the most important ideas are reviewed here. We assume a rigid-ion model and calculate the band structure with the empirical local-pseudopotential method. All phonons $\mathbf{Q},j$ ($\mathbf{Q}\equiv$wave vector, $j=$branch) contribute to the energy shift $\Delta E_{\mathbf{k}n}$:

$$\Delta E_{\mathbf{k}n}(T) = \sum_{\mathbf{Q},j} \left[\frac{\partial E_{\mathbf{k}n}}{\partial n_{\mathbf{Q}j}}\right][n_{\mathbf{Q}j}(T)+\tfrac{1}{2}], \tag{3}$$

where $n_{\mathbf{Q}j}$ is the occupation number of the phonon mode. By introducing a temperature-independent electron-phonon spectral function g^2F,

$$g^2F(\mathbf{k},n;\Omega)=\sum_{\mathbf{Q},j}\left[\frac{\partial E_{\mathbf{k}n}}{\partial n_{\mathbf{Q}j}}\right]\delta(\Omega-\omega_{\mathbf{Q}j}) , \tag{4}$$

with $\omega_{\mathbf{Q}j}$ the phonon energy, one has

$$\Delta E_{\mathbf{k}n}(T)=\int_0^{\omega_{\max}} d\Omega\, g^2F(\mathbf{k},n;\Omega)[(e^{\Omega/T}-1)^{-1}+\tfrac{1}{2}] . \tag{5}$$

The total contribution to the spectral function from phonon $\mathbf{Q},j$ is the sum of the Debye-Waller (DW) and self-energy (SE) contributions, given by

$$\left[\frac{\partial E_{\mathbf{k}n}}{\partial n_{\mathbf{Q}j}}\right]_{\mathrm{SE}}=\tfrac{1}{2}\sum_{n'}\frac{[\mathbf{\Gamma}(\mathbf{k},n,n';\mathbf{Q})\cdot\mathbf{u}(\mathbf{Q},j;+)+\mathbf{\Theta}(\mathbf{k},n,n';\mathbf{Q})\cdot\mathbf{u}(\mathbf{Q},j;-)]^2}{\epsilon_{\mathbf{k}n}-\epsilon_{\mathbf{k}+\mathbf{Q},n'}} , \tag{6}$$

$$\left[\frac{\partial E_{\mathbf{k}n}}{\partial n_{\mathbf{Q}j}}\right]_{\mathrm{DW}}=-\tfrac{1}{2}\sum_{n'}\frac{[\mathbf{\Gamma}(\mathbf{k},n,n';\mathbf{0})\cdot\mathbf{u}(\mathbf{Q},j;+)^2+\mathbf{\Gamma}(\mathbf{k},n,n';\mathbf{0})\cdot u(\mathbf{Q},j;-)]^2}{\epsilon_{\mathbf{k}n}-\epsilon_{\mathbf{k}n'}} . \tag{7}$$

$\epsilon_{\mathbf{k}n}$ is the electron energy in state $\mathbf{k},n$. The displacements $u(\pm)$ are the even and odd combinations of displacement of the two atoms in the unit cell which are easily obtained from the phonon eigenvectors. The βth component of $\mathbf{\Gamma}$ was evaluated to be[6]

$$\Gamma_\beta(\mathbf{k},n,n';\mathbf{Q})\equiv\sum_{\mathbf{G},\mathbf{G}'}C_{\mathbf{k}+\mathbf{Q},n'}(\mathbf{G}')C_{\mathbf{k}n}(\mathbf{G})(\mathbf{G}'-\mathbf{G}+\mathbf{Q})_\beta V(\mathbf{G}'-\mathbf{G}+\mathbf{Q})\cos[(\mathbf{G}'-\mathbf{G})\cdot\boldsymbol{\tau}] ; \tag{8}$$

Θ_β is the same as Γ_β, except the cosine is replaced by the sine. The electronic wave functions $C_{\mathbf{k}n}(\mathbf{G})$ are eigenvectors of the secular equation

$$\begin{aligned}0&=\sum_{\mathbf{G}}\{[(\mathbf{k}+\mathbf{G})^2-\epsilon_{\mathbf{k}n}]\delta_{\mathbf{G}\mathbf{G}'}\\&\quad+V(\mathbf{G}-\mathbf{G}')S(\mathbf{G}-\mathbf{G}')\}C_{\mathbf{k}n}(\mathbf{G}') ,\\ \psi_{\mathbf{k}n}&=\Omega^{-1/2}\sum_{\mathbf{G}}C_{\mathbf{k}n}(\mathbf{G})e^{i(\mathbf{k}+\mathbf{G})\cdot\mathbf{r}} ,\\ \sum_{\mathbf{G}}&|C_{\mathbf{k}n}(\mathbf{G})|^2=1 ,\end{aligned} \tag{9}$$

where $V(\mathbf{G})$ is the local-pseudopotential form factor and $S(\mathbf{G})$ is the structure factor given by $S(G)=\cos(\mathbf{G}\cdot\boldsymbol{\tau})$, with $\boldsymbol{\tau}=\boldsymbol{\tau}_1=-\boldsymbol{\tau}_2$, $\boldsymbol{\tau}_1$ and $\boldsymbol{\tau}_2$ being the locations of the two atoms in the primitive cell.

III. NUMERICAL CALCULATIONS

The spectral functions $g^2F(\mathbf{k},n;\Omega)$ were computed for valence- and conduction-band states with the use of the tetrahedron method.[7] The irreducible $\frac{1}{48}$th wedge of the Brillouin zone (BZ) was divided into 228 small tetrahedra which correspond to a discrete mesh of 89 $\mathbf{k}$ points. To calculate the phonon frequencies and eigenvectors, the bond-charge—model[8] programs[9] of Weber were used. The band structure was determined from Eq. (9) using Cohen-Bergstresser[10] pseudopotential form factors. Equation (8) requires knowledge of $V(\mathbf{Q})$ for $\mathbf{Q}$ not equal to a reciprocal-lattice vector $\mathbf{G}$. We tested both extrapolations shown in Fig. 1 of paper II and found the resulting $\Delta E(T)$ to differ by less than 2% for the Si E_0' gap. All calculations reported here use the potential V_B of II, which is extrapolated to $V(\mathbf{0})=-2\epsilon_F/3$.

In Eq. (6) a sum must be performed over the intermediate states n'. After some tests concerning the contributions of higher intermediate states, the sum was restricted to $n'=30$ in order to save computer time. Some error is also introduced in the electron-state eigenvectors because of the truncation of the Hamiltonian matrix to 59 plane waves. The sum of these truncation errors is estimated to be less than 5%.

With the present computer program it is possible to calculate the renormalization of band energies by electron-phonon interaction for electronic states $\mathbf{k},n$ at any point of the BZ. In order to compare the results with present experimental data, the calculations were done for several optical transitions in Si and Ge: the indirect gap ($\Gamma_{25'}\rightarrow L_1$ in Ge, $\Gamma_{25'}\rightarrow 0.84X_1$ in Si), the second direct gap ($\Gamma_{25'}\rightarrow\Gamma_{15}$ or E_0' gap in Ge, $\Gamma_{25'}\rightarrow\Gamma_{2'}$ or E_0 gap in Si), the E_1 gap [transitions $\Lambda_3\rightarrow\Lambda_1$ between $(2\pi/a)\langle\frac{1}{4},\frac{1}{4},\frac{1}{4}\rangle$ and $(2\pi/a)\langle\frac{1}{2},\frac{1}{2},\frac{1}{2}\rangle$], and the E_2 gap. The region where the E_2 transitions take place is not very well defined. We use the points $(2\pi/a)(0.9,0.1,0.1)$ for Si and $(2\pi/a)(\frac{3}{4},\frac{1}{4},\frac{1}{4})$ for Ge as representative points.[11]

Only for the initial $\mathbf{k}$ states at the Γ point can the $\mathbf{Q}$-sum in Eq. (4) be restricted to the irreducible wedge of the BZ. For a general $\mathbf{k}$ point the sum can also be carried out over the irreducible part of the BZ, provided one sums up the contributions of all vectors in the star of $\mathbf{k}$ in order to obtain g^2F. For instance, for a $\mathbf{k}$ point along the Λ line, the $\mathbf{Q}$ sum in Eq. (4) was carried out in the $\frac{1}{48}$th wedge of the BZ for the eight points in the star of $|\mathbf{k}|[1,1,1]$ and added.

For one initial state and one point of a star, the calculations took about 45 min of central processing unit (CPU) time on a Honeywell-Bull 66-80P computer. This means that for a transition along Λ with three initial states (twofold-degenerate valence band, onefold-degenerate conduction band) and eight points of the star of $\mathbf{k}$, the calculation took about 18 h of CPU time for one $\mathbf{k}$ point along Λ.

A problem arose concerning the accuracy of the electron-energy and eigenvector calculations at $\mathbf{k}+\mathbf{Q}$ points outside the first BZ [Eq. (8)]. The summation in the secular equation [Eq. (9)] is limited to 59 reciprocal-

lattice vectors $\mathbf{G}$, which correspond to all $\langle 000\rangle$, $\langle 111\rangle$, $\langle 200\rangle$, $\langle 220\rangle$, $\langle 311\rangle$, and $\langle 222\rangle$ plane waves. This set of plane waves is closed with respect to the point-group operations. At a point $\mathbf{k}$ near the zone edge, however, the set $\langle \mathbf{G}+\mathbf{k}\rangle$ is not closed: some operations of the group of $\mathbf{k}$ transform some $\mathbf{G}+\mathbf{k}$'s into $\mathbf{G}'+\mathbf{k}$, where $\mathbf{G}'$ has been truncated away in our original Hamiltonian. As a result, some of the symmetry-imposed degeneracies at the BZ edge are missing. The errors become larger the larger the $\mathbf{k}$, particularly outside of the BZ. Since electron-phonon coupling can take us from inside to outside the BZ, the problem just discussed can introduce large errors for phonons of large $\mathbf{Q}$. This problem can be reduced by bringing all states outside of the first BZ to the first BZ through addition of a reciprocal-lattice vector $\overline{\mathbf{G}}$. Hence, instead of Eq. (8), we use

$$\Gamma_\beta(\mathbf{k},n,n';\mathbf{Q}) \equiv \sum_{\mathbf{G}',\mathbf{G}} C_{\mathbf{k}+\mathbf{Q}+\overline{\mathbf{G}},n'}(\mathbf{G}')C_{\mathbf{k}n}(\mathbf{G})(\mathbf{G}'+\overline{\mathbf{G}}-\mathbf{G}+\mathbf{Q})_\beta V(\mathbf{G}'+\overline{\mathbf{G}}-\mathbf{G}+\mathbf{Q})\cos[(\mathbf{G}'+\overline{\mathbf{G}}-\mathbf{G})\cdot\tau] \,. \tag{10}$$

To check the numerical procedure, tests were performed as described in II and Ref. 6.

One sensitive check is the direct calculation of the Debye-Waller effect. In the secular equation (9) the zero-temperature structure factor $S(\mathbf{G})$ can be replaced by[1]

$$S(\mathbf{G})\exp(-\tfrac{1}{6}|\mathbf{G}|^2\langle u^2\rangle) \,, \tag{11}$$

where $\langle u^2\rangle$ is the mean-square displacement of the atom. By doing band-structure calculations with this temperature-dependent structure factor, the shifts of the gaps agree with the result obtained by perturbation theory within a few percent (e.g., 3% for Si, $\Gamma_{25'}$ state). Furthermore, the electron-phonon selection rules have been tested for electron transitions from X to Γ, L to Γ, and for one point on Λ to Γ and Δ to Γ, respectively. The corresponding selection rules are strictly obeyed.

IV. RESULTS

As an example, for the calculated spectral functions $g^2F(\Omega)$, two sequences of these functions are shown in Figs. 1 and 2 for initial states along the Λ direction of Si, including those for the Γ and L points.

The highest valence-band states (Fig. 1) show, with increasing separation from the Γ point, an increasing contribution from the acoustic phonons, which remains nearly constant from midway to the L point. On the other hand, the contributions from the high-energy optical phonons which are located in the region around the Γ point decrease. This is due to the larger energy denominators in Eqs. (6) and (7). The behavior of the conduction-band states can be seen in Fig. 2. Here the spectral functions $g^2F(\Omega)$ are negative, except for the acoustic phonons at

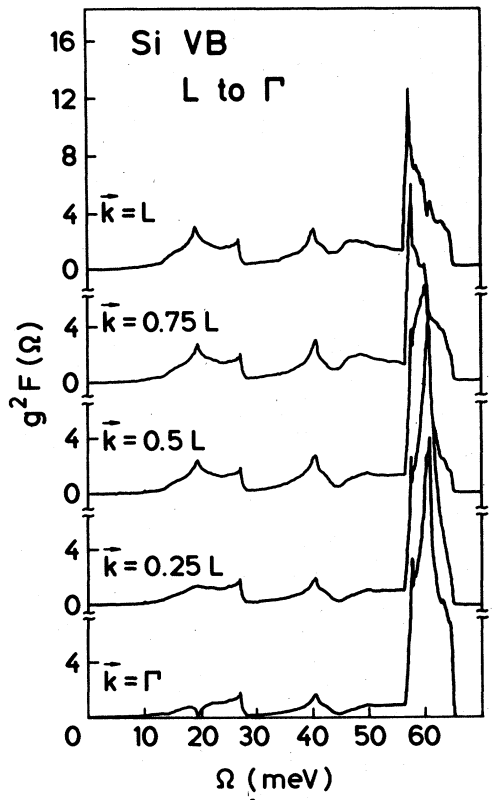

FIG. 1. Spectral functions $g^2F(\Omega)$ for the highest valence-band state (VB) of Si. A sequence of $\mathbf{k}$ points from from L to Γ is shown.

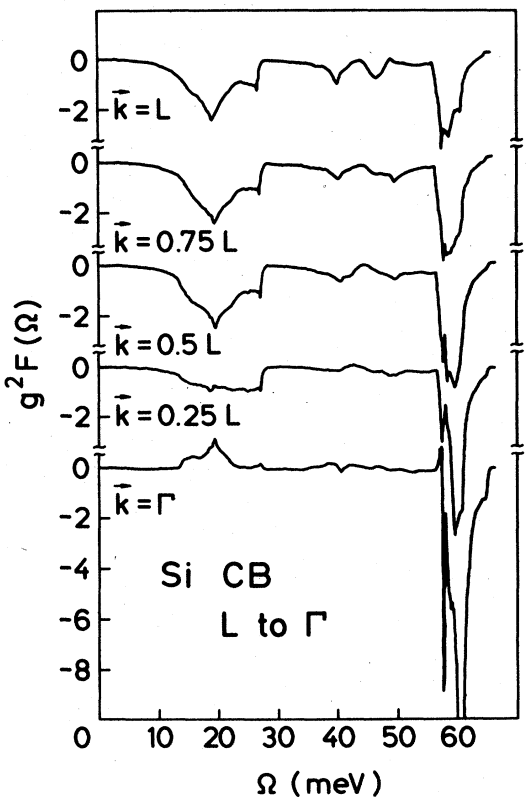

FIG. 2. Spectral functions $g^2F(\Omega)$ for the lowest conduction-band state (CB) of Si. A sequence of points from L to Γ is shown.

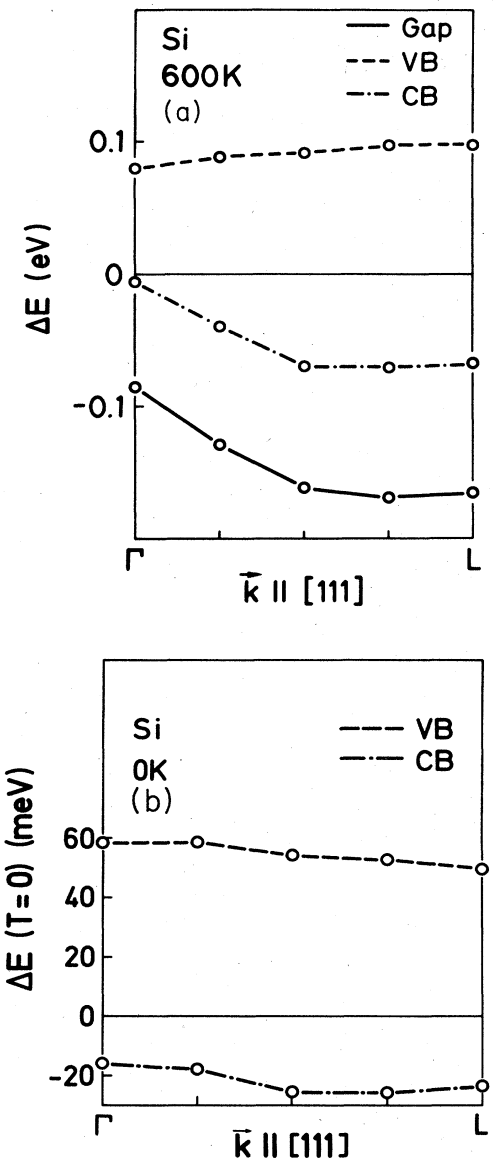

FIG. 3. (a) Energy shifts of states along the Λ direction for Si for a change of temperature from 0 to 600 K due to electron-phonon interaction. The lines are guides for the eye. Dashed line: shift for states at the highest valence band (VB). Dotted-dashed line: shift for states of lowest conduction band (CB). Solid line: total shift to lower energies of the band gap (Gap). (b) Zero-point shift $\Delta E(0)$ for Si (in meV). The notation is the same as in (a).

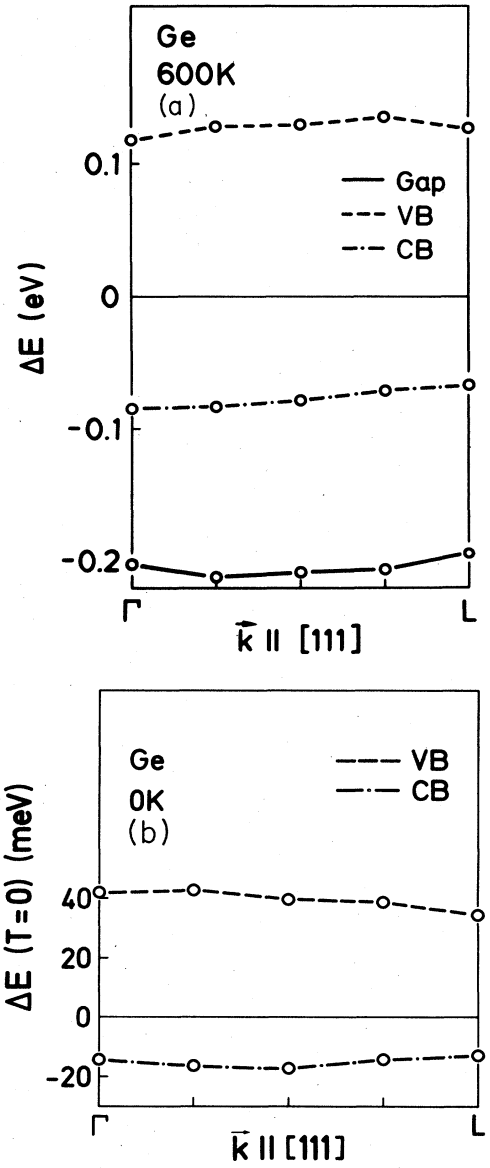

FIG. 4. (a) Energy shifts of states along the Λ direction for Ge for a change of temperature from 0 to 600 K due to electron-phonon interaction [the notation is explained in Fig. 3(a)]. (b) Zero-point shift of $\Delta E(0)$ for Ge (in meV). The notation is the same as in Fig. 3(a).

the Γ point. With increasing distance from Γ in the Λ direction, this contribution also becomes negative, again remaining nearly constant from $\Lambda=0.5L$ to the L point. Also, the peak due to the optical phonons decreases.

In order to see the resulting dispersion of the temperature shift of the states along the Λ line, Fig. 3 shows the shift of the valence- and conduction-band states as well as the total shift of the gap for a change of temperature chosen to be from 0 to 600 K for Si. These shifts were obtained by means of Eq. (3) after integration of $g^2F(\Omega)$. There is a shift of the energy even at $T=0$. These zero-point shifts, however, are subtracted out in Fig. 3(a) and shown separately in Fig. 3(b).

The valence-band shift in Fig. 3(a) increases very slightly when moving from Γ towards L. there is, from Γ to L, an increasing contribution of the acoustic phonons (Fig. 1) which is only partially compensated for by the decrease in the contribution of the optical phonons. The slight negative conduction-band shift at Γ becomes more negative with the increasing negative acoustic part of the spectral function until about $0.5L$. The resulting negative shift of the gap shows basically the same **k** dispersion as that of

the conduction band. The zero-point shifts of the conduction and valence band in Fig. 3(b) show only slight changes along the Λ line. These shifts $\Delta E(0)$ are proportional to the area under $g^2F(\Omega)$: the area under the spectral functions remains nearly constant, although there are changes in their shapes.

In Fig. 4(a) we show the corresponding results for Ge, again the shift of the electronic states for a change of temperature from 0 to 600 K. In this case, the shifts show much less dispersion. However, because of the bowing of the conduction band between $0.25L$ and Γ, no direct comparison to the case of Si can be made (note that the ordering of the $\Gamma_{2'}$-Γ_{15} conduction bands reverses from Ge to Si). The zero-point shifts, displayed in Fig. 4(b), are again almost constant, but lower in magnitude than those for silicon. This is, in part, a consequence of the smaller zero-point vibrational amplitude of germanium which follows from its higher atomic mass.

The temperature shifts of several selected states in the BZ, from which some gaps and critical points arise, are shown in Figs. 5 and 6 for Si and Ge. These shifts include Debye-Waller and self-energy terms, but not the thermal-expansion effect. The zero-point shift $\Delta E(0)$ is proportional to the area under $g^2F(\Omega)$; however, in the high-temperature limit there is a factor $2k_BT/\hbar\Omega$ in the integrand which weights the acoustic phonons more than the optic ones. Hence, the large shifts of the $\Gamma_{25'}$ and $L_{3'}$ in Si and Ge, and $\Gamma_{2'}$ in Si, indicate large acoustic phonon contributions. The $0.84X$ conduction-band state of Si and the Γ_{15} state of Ge show small shifts, but this is due to the fact that a positive shift by the acoustic phonons is partly cancelled by a negative shift by the optical phonons.

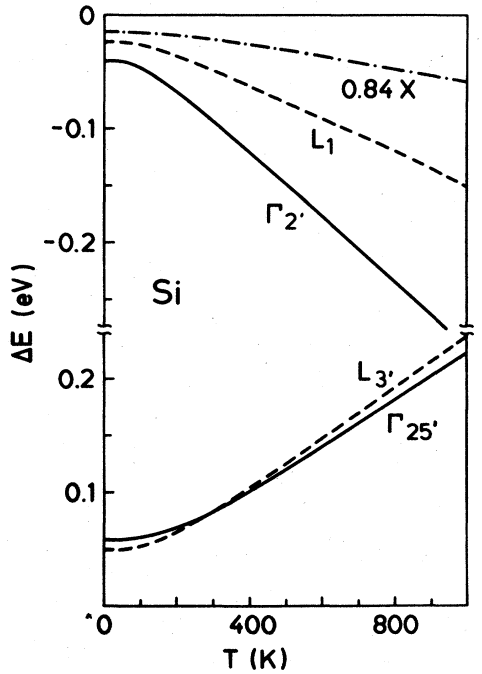

FIG. 5. Temperature-dependent shift $\Delta E_{kn}(T)$ of states at the Γ, L, and $0.84X$ points of Si. The shifts at $T=0$ originate from zero-point renormalizations due to electron-phonon interaction.

V. SHIFT OF GAPS AND CRITICAL POINTS

Let us now focus our attention on the temperature shift of the various gaps and critical points in Si and Ge, and compare them with present experimental data. As already mentioned [Eq. (1)], the temperature shift from electron-phonon interaction and the contribution from thermal expansion must be added to obtain the total thermal shift.

In Table I the values for the calculation of $(\partial E/\partial T)_{\text{therm exp}}$ are listed. The linear thermal-expansion coefficient is temperature dependent; for the calculation we used the thermal-expansion data of Ref. 12.

A. Indirect gap

The transitions of the indirect gap take place between the top of the valence band $\Gamma_{25'}$ and the valleys located at about $\mathbf{k}=(2\pi/a)(0.84,0,0)$ for Si and $\mathbf{k}=(\pi/a)(1,1,1)$ for Ge. The shifts of these gaps with temperature are shown in Fig. 7, in the upper part for Si and in the lower for Ge. The dashed curves give the contribution of the electron-phonon interaction and the solid curves give that of the total shifts including thermal-expansion effects. The total shift of the indirect gap of Si is smaller than the electron-phonon effect because of the negative pressure coefficient of the indirect gap.[13] The dotted curves are from the experimental data of MacFarlane *et al.*,[14,15] which were fitted by Thurmond[16] with the expression first proposed by Varshni,[17]

$$\Delta E(T)=\alpha T^2/(T+\beta)\ . \tag{12}$$

The experimental data are only available from 0 to 400 K. The theoretical and experimental values show very good

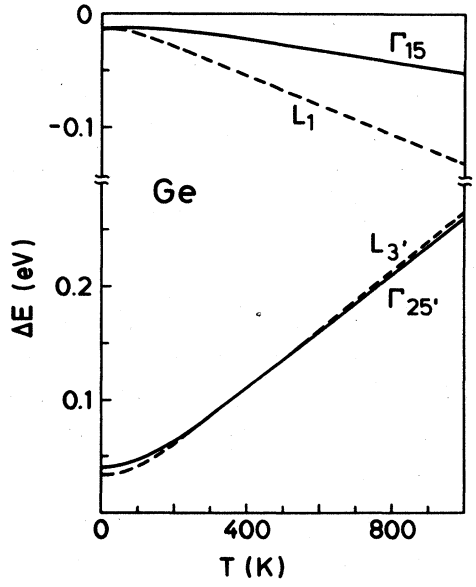

FIG. 6. Temperature-dependent shift $\Delta E_{kn}(T)$ of states at the Γ and L points of Ge.

TABLE I. Data for the calculation of the thermal shift of band gaps $(\Delta E)_{\text{therm exp}} = -3B(\partial E_g/\partial p)_T \int_0^T \alpha\, dT$.

		Si			Ge	
B (10^{11} N/m^2)			0.98[b]			0.75[b]
$(\partial E/\partial p)_T$ (10^{-6} eV/bar)	$\Gamma_{25'}$-$\Gamma_{2'}$	E_0	11.6[a]	$\Gamma_{25'}$-Γ_{15}	E_0'	0.8[a]
	$\Gamma_{25'}$-0.84X_1	E_{ind}	−1.6[a]	$\Gamma_{25'}$-L_1	E_{ind}	4.6[a]
	Λ_3-Λ_1	E_1	5.2[b]	Λ_3-Λ_1	E_1	7.5[b]
		E_2	2.9[b]		E_2	5.6[b]
α	temperature dependent, $\int_0^T \alpha\, dT$ obtained from data of Ref. 12.					

[a]Reference 13.
[b]Reference 12.

agreement for Ge. For Si, however, there is a discrepancy of about 40 meV (25%) in the shift for 400 K.

B. Second direct gaps

The second-lowest gaps correspond to transitions between $\Gamma_{25'}$-$\Gamma_{2'}$ in Si and $\Gamma_{25'}$-Γ_{15} in Ge. In Fig. 8 the calculated temperature shifts are shown. Only two experimental points are drawn in for Si, measured by electroreflectance by Aspnes and Studna[18] at 4.2 and 190 K. At higher temperatures the E_0 structure cannot be resolved because of the dominating E_2 structure, which is close by. The experimental curve for Ge is from recent measurements by Viña *et al.*[19] obtained by averaging the energies of the E_0 and $E_0+\Delta_0$ transitions. In this case a very good agreement between experiment and theory is obtained.

C. E_1 critical points

The total shifts of the E_1 transitions are taken to be the average of those for $\mathbf{k}=(\pi/2a)(1,1,1)$, $\mathbf{k}=(3\pi/4a)(1,1,1)$, and $\mathbf{k}=(\pi/a)(1,1,1)$. Figure 9 again shows the calculated electron-phonon shifts and the total shift (electron phonon plus thermal expansion, solid lines). The two dots are experimental values for Si from Daunois and Aspnes.[20] The dotted curve for Si is derived from temperature-dependent ellipsometric measurements of the optical constants by Jellison and Modine.[21] They labeled the peak near 3.4 eV in the measured real part of the dielectric function ϵ_1 as E_0' and thought it to arise from $\Gamma_{25'}$-Γ_{15} transitions, while the peak in ϵ_2 was attributed to the E_1 transitions. Following the current ideas, we believe that both these peaks arise mainly from transitions of the E_1 type: as recently shown for Ge,[19] the E_0' structure should be much weaker

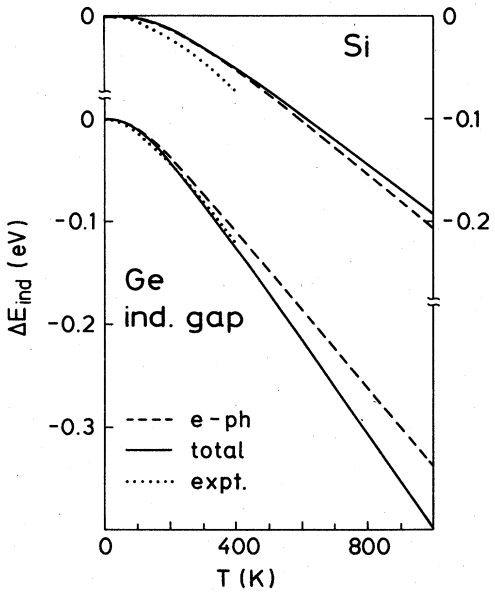

FIG. 7. Shift of the indirect gaps of Si (upper part) and Ge (lower part) vs temperature. Dashed line: shift due to electron-phonon interaction. Solid line: total shift, including contribution of electron-phonon interaction and thermal-expansion effect. Dotted line: experimental results from Ref. 16.

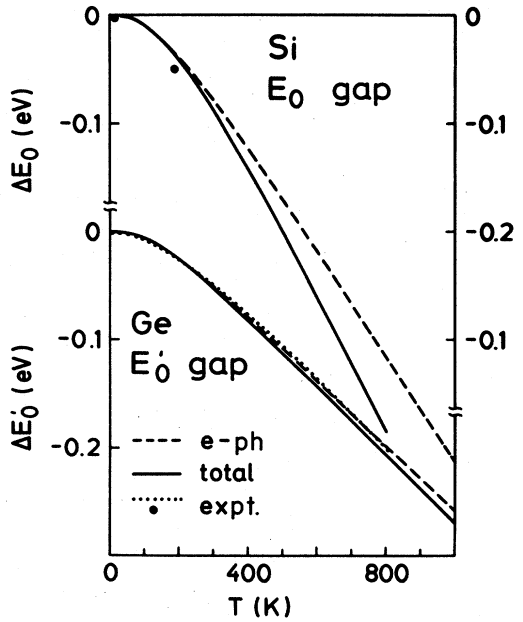

FIG. 8. Shift of the E_0 gap of Si and E_0' gap of Ge vs temperature. Dashed line: shift due to electron-phonon interaction. Solid line: shift due to electron-phonon interaction plus thermal-expansion effect. Dots: experimental points from Ref. 18. Dotted line: experimental results from Ref. 19.

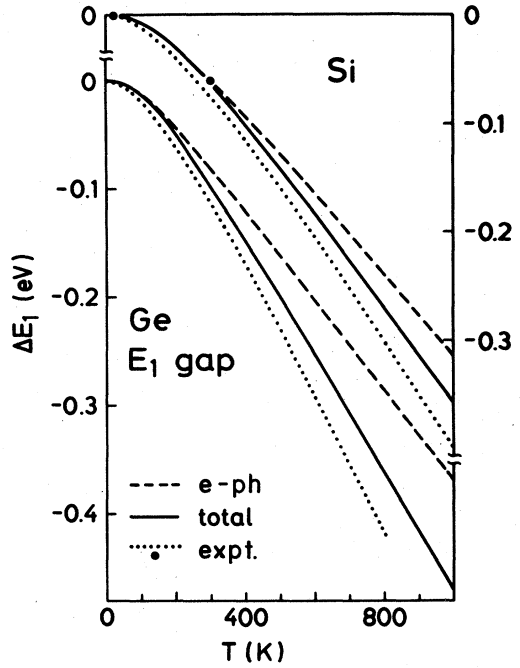

FIG. 9. Shift of the E_1 gap of Si and Ge vs temperature. Dashed line: shift due to electron-phonon interaction. Solid line: shift due to electron-phonon interaction plus thermal-expansion effect. Dots: experimental points from Ref. 20. Dotted line: experimental results from Refs. 21 (for Si) and 19 (for Ge).

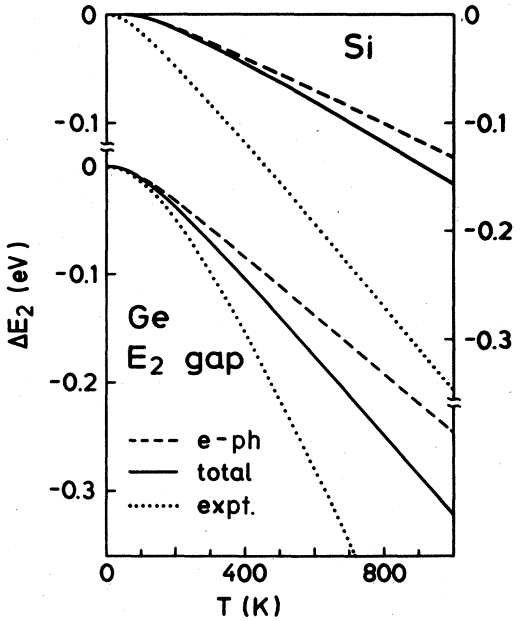

FIG. 10. Shift of the E_2 gap of Si and Ge vs temperature. Dashed line: shift due to electron-phonon interaction. Solid line: shift due to electron-phonon interaction plus thermal-expansion effect. Dotted line: experimental results from Refs. 21 (for Si) and 19 (for Ge).

than the E_1 counterpart, as follows from phase-space arguments. To obtain the temperature dependence of this transition, Jellison and Modine plotted the peak position of the features in ϵ_1 as a function of temperature. The critical-point energy should not occur exactly at the top of either peak in ϵ_1 or ϵ_2.[20,21] In the absence of a line-shape analysis of these peaks, of the type performed in Ge,[19] we assume that the E_1 critical point is close to the maximum in ϵ_1. This assumption follows from the fact that the peak in ϵ_1 is nearly symmetric, while the corresponding peak in ϵ_2 exhibits considerable asymmetry.

The resulting temperature shift up to about 1000 K was fitted to Varshni's relation [Eq. (12)]. The shift is even slightly larger than the calculated shift, another hint that the experimental peak in ϵ_1 is more related to an E_1 critical point, because the E_0' gap in Si shows a much lower temperature dependence (see II).

For Ge, a good agreement with the experimental results of Viña *et al.*[19] is obtained. These data were obtained through careful analysis of the line shape of the critical point by fitting the second derivative of the dielectric functions to theoretical line shapes.

D. E_2 critical points

The temperature shift of the E_2 gaps is shown in Fig. 10. As the representative points for these transitions, we used $\mathbf{k}=(2\pi/a)(0.9,0.1,0.1)$ for Si,[10] and $\mathbf{k}=(2\pi/a)(0.75,0.25,0.25)$ for Ge.[11] Again, the dotted curves show the experimental data. For Si we took, as the E_2 energy, the peak in the imaginary part of the dielectric function, measured by Jellison and Modine[21] and fitted by the Varshni equation, (12). This peak is more symmetric than the structure in ϵ_1.

For Ge we took advantage of the analysis of the critical-point energies done by Viña *et al.*[19] These authors found that a two-dimensional critical point yields the best representation of the E_2 structure over the entire temperature range. Their results are described by the corresponding dotted line in Fig. 10.

As seen in Fig. 10, in the case of the E_2 transitions there is a considerable discrepancy between the calculated and experimental temperature shifts. The relative discrepancy is particularly large for Si. A better agreement is obtained with experimental data from reflectivity measurements[22,19] (see Table II), but as already pointed out,[19] shifts and broadenings appear mixed in the temperature coefficient, so that a line-shape analysis should be more accurate. The fact that this analysis has not been performed for silicon may explain the corresponding discrepancy in Fig. 10. A qualitative analysis of Fig. 1 of Ref. 21 suggests that one may have to reduce the experimental shifts for Si in Fig. 10 by as much as 30%. Some discrepancy may also result from uncertainties in the location of the E_2 critical points in $\mathbf{k}$ space.

VI. DISCUSSION

It is customary to fit the experimental data on the temperature dependence of gaps with the empirical relation of Eq. (12), as suggested by Varshni.[16] However, it is also

TABLE II. Linear temperature coefficients of interband transitions in Si and Ge in units of 10^{-4} eV/K. $(\Delta E_g/\Delta T)_V$ are the calculated contributions from electron-phonon interaction. $(\Delta E_g/\Delta T)_{\text{tot}}$ is the total shift, including the effect by thermal expansion. The values are shown for the temperature ranges 200—300 and 600—800 K, and are compared with experimental results.

	Si				Ge			
	200—300 K		600—800 K		200—300 K		600—800 K	
	Calc.	Expt.	Calc.	Expt.	Calc.	Expt.	Calc.	Expt.
E_0 gap $(\Delta E_0/\Delta T)_V$	−4.0		−4.9		−3.8		−4.2	
$(\Delta E_0/\Delta T)_{\text{tot}}$	−4.7		−6.2		−5.4	−4.2[f]	−6.4	−5.9[f,c]
E_0' gap $(\Delta E_0'/\Delta T)_V$	−1.5		−2.3		−2.6		−3.0	
$(\Delta E_0'/\Delta T)_{\text{tot}}$	−1.5		−2.4		−2.7	−2.4[g]	−3.1	−3.2[g]
E_{ind} gap $(\Delta E_{\text{ind}}/\Delta T)_V$	−1.8		−2.6		−3.4		−3.8	
$(\Delta E_{\text{ind}}/\Delta T)_{\text{tot}}$	−1.7	−2.3[a]	−2.4	−4.3[a,c]	−4.0	−3.6[f]	−4.6	−4.3[a,c]
		−2.3[b]		−3.6[b,c]		−3.6[h]		−4.5[b,c]
E_1 gap $(\Delta E_1/\Delta T)_V$	−3.0		−3.7		−3.8		−4.1	
$(\Delta E_1/\Delta T)_{\text{tot}}$	−3.3	−2.2[d]	−4.3	−4.7[e]	−4.7	−4.2[d]	−5.4	−6.3[g]
		−3.6[e]				−5.1[g]		
E_2 gap $(\Delta E_2/\Delta T)_V$	−1.3		−1.5		−2.5		−2.7	
$(\Delta E_2/\Delta T)_{\text{tot}}$	−1.5	−2.2[d]	−1.8	−3.8[e]	−3.2	−4.7[g] (2D)[i]	−3.7	−6.9[g] (2D)[i]
		−3.5[e]				−4.6[g] (1D)[i]		−6.1[g] (1D)[i]
						−2.4[d]		

[a]Data of MacFarlane *et al.* (Ref. 14) fitted by Varshni (Ref. 17).
[b]Data of MacFarlane *et al.* (Ref. 14) refitted by Thurmond (Ref. 16).
[c]Empirical formula by Varshni [Eq. (12)] extrapolated to higher temperatures.
[d]Reference 22.
[e]Reference 21.
[f]Reference 17.
[g]Reference 19.
[h]Reference 16.
[i]Assumption of a two- (2D) or one-dimensional (1D) critical point for E_2.

possible to fit the data with an expression involving a gap shift proportional to Bose-Einstein statistical factors for phonon emission and absorption, as shown in Ref. 19 for the (80—800)-K range. The only significant difference between these fits occurs at low temperatures ($T<80$ K), where only few experimental data are available. Accurate measurements below 80 K, particularly for the E_1 gaps, are desirable in order to check with expression fits better.

With the computer program used for the present calculations, it is not possible to describe the low-temperature behavior very accurately. At low temperature the only contribution to the temperature shift is due to low-energy acoustic phonons. Our mesh, chosen to consist of 89 points in the $\frac{1}{48}$th wedge of the Brillouin zone, is too coarse, since only few mesh points near Γ contribute at low temperatures. Besides, the phonon energies are not isotropic, so that it is necessary to consider all directions of the irreducible part of the zone. The first small tetrahedron, with a corner at the Γ point, contributes mainly to the low-temperature behavior. For this tetrahedron our calculation interpolates between only three directions of the BZ. This interpolation may not properly describe the strong anisotropy of the acoustic phonons near $\mathbf{Q}=\mathbf{0}$ in the irreducible part of the zone. In view of this we believe that our calculations cannot, at this point, distinguish between the Varshni expression and the Bose-Einstein temperature dependence used in Ref. 19. However, at higher temperatures the results become more accurate. In Table II we list the average temperature coefficients of all investigated gaps of Si and Ge. These coefficients also depend on temperature—values are given for temperatures between 200 and 300 K as well as for 600—800 K. For comparison, the experimental values are listed. The lowest direct gaps (E_0' for Si, E_0 for Ge) have already been treated in II.

The E_0' gap of Si is nearly degenerate with the E_1 gap, but shows a much lower temperature shift. Despite this difference, there is no experiment resolving the E_0' and E_1 transitions at various temperatures.

We should mention that a rising temperature not only shifts gaps and critical points but also broadens them. Lorentzian broadening parameters versus temperature have been recently determined for several interband critical points of Ge.[19] The phonon-induced broadenings arise from the same mechanism which determines the real parts of the self-energy. Their evaluation requires a separate double Brillouin-zone integration (one for intermediate electronic states and one for phonons). Results of these calculations and comparison with experimental data will be published elsewhere.

ACKNOWLEDGMENTS

Thanks are due S. Logothetidis and L. Viña for making their experimental data available prior to publication and for a number of discussions. One of us (P.B.A.) thanks the A. von Humboldt Foundation for support, and also acknowledges support from the U.S. National Science foundation under Grant No. DMR-81-21954-A01.

---

*Permanent address: Department of Physics, State University of New York at Stony Brook, Stony Brook, NY 11794.

[1]M. L. Cohen and D. J. Chadi, in *Semiconductor Handbook,* edited by M. Balkanski (North-Holland, Amsterdam, 1980), Vol. 2, chap. 4b.

[2]E. Antoncik, Czech. J. Phys. **5**, 449 (1955).

[3]H. Y. Fan, Phys. Rev. **82**, 900 (1951).

[4]P. B. Allen and V. Heine, J. Phys. C **9**, 2305 (1976).

[5]P. B. Allen and M. Cardona, Phys. Rev. B **27**, 4760 (1983) (hereafter denoted II).

[6]P. B. Allen and M. Cardona, Phys. Rev. B **23**, 1495 (1981); **24**, 7479 (1981).

[7]G. Lehmann and M. Taut, Phys. Status Solidi B **54**, 469 (1972); **57**, 815 (1973).

[8]W. Weber, Phys. Rev. B **15**, 4789 (1977).

[9]O. H. Nielsen and W. Weber, Comput. Phys. Commun. **18**, 101 (1979).

[10]M. L. Cohen and T. K. Bergstresser, Phys. Rev. **141**, 789 (1966).

[11]J. R. Chelikowsky and M. L. Cohen, Phys. Rev. B **14**, 556 (1976); Phys. Rev. Lett. **31**, 1582 (1973).

[12]*Landolt-Börnstein Tables, Group III,* Vol. 17a of *Physics of Group IV Elements and III-V Compounds,* edited by O. Madelung (Springer, Berlin, 1982).

[13]K. J. Chang, S. Froyen, and M. L. Cohen, Solid State Commun. **50**, 105 (1984).

[14]G. G. MacFarlane, T. P. McLean, J. E. Quarrington, and V. Roberts, Phys. Rev. **111**, 1245 (1958).

[15]G. G. MacFarlane, T. P. McLean, J. E. Quarrington, and V. Roberts, Phys. Rev. **108**, 1377 (1957).

[16]C. D. Thurmond, J. Electrochem. Soc. **122**, 1133 (1975).

[17]K. P. Varshni, Physica (Utrecht) **34**, 149 (1967).

[18]D. E. Aspnes and A. A. Studna, Solid State Commun. **11**, 1375 (1972).

[19]L. Viña, S. Logothetidis, and M. Cardona, Phys. Rev. B **30**, 1979 (1984).

[20]A. Daunois and D. E. Aspnes, Phys. Rev. B **18**, 1824 (1978).

[21]G. E. Jellison, Jr. and F. A. Modine, Phys. Rev. B **27**, 7466 (1983).

[22]R. R. L. Zucca and Y. R. Shen, Phys. Rev. B **1**, 2668 (1970).